UNIVERSITY OF BATH

University of Bath

Article

Structural and functional analysis of anti-influenza activity of 4-, 7-, 8- and 9-deoxygenated 2,3-difluoro-N-acetylneuraminic acid derivatives

Jennifer Lois McKimm-Breschkin, Susan Barrett, Patricia A. Pilling, Stefan Hader, Andrew G Watts, and Victor A Streltsov

Just Accepted

Structural and functional analysis of anti-influenza activity of 4-, 7-, 8- and 9-deoxygenated

2,3-difluoro-N-acetylneuraminic acid derivatives

Authors

Jennifer L. McKimm-Breschkin[a,*], Susan Barrett[a], Patricia A. Pilling[a], Stefan Hader[b], Andrew G.

Watts[b] and Victor A. Streltsov[c]

Affiliations

[a] CSIRO Manufacturing, 343 Royal Parade, Parkville, 3052 Australia

[b] Department of Pharmacy and Pharmacology, University of Bath, Claverton Down, Bath BA2

7AY, United Kingdom

[c] The Florey Institute of Neuroscience and Mental Health, 30 Royal Parade, Parkville, VIC 3052,

Australia

*Corresponding author

Jennifer L McKimm-Breschkin

jmbvirology@gmail.com

Phone +613 8344 1106

Abstract

Competitive inhibitors of the influenza neuraminidase (NA) were discovered almost 20 years

ago, with zanamivir and oseltamivir licensed globally. These compounds are based on a

transition state analogue of the sialic acid substrate. We recently showed that 5-(Acetylamino)-

2,3,5-trideoxy-2,3-difluoro-D-erythro-β-L-manno-2-nonulopyranosonic acid (DFSA) and its

derivatives are also potent inhibitors of the influenza NA. They are mechanism based inhibitors,

forming a covalent bond between the C2 of the sugar ring and Y406 in the NA active site, thus

inactivating the enzyme. We have now synthesized a series of deoxygenated DFSA derivatives

in order to understand the contribution of each hydroxyl in DFSA to binding and inhibition of the

influenza NA. We have investigated their relative efficacy in enzyme assays *in vitro*, in cell

culture and by X-ray crystallography. We found loss of the 8- and 9-OH had the biggest impact

on the affinity of binding and antiviral potency.

2

1. Introduction

There are two types of influenza which cause significant morbidity and mortality in humans, influenza A and B. Both influenza A and B viruses have two surface glycoproteins, the hemagglutinin (HA) responsible for binding to sialic acid containing receptors on the cell surface, and the neuraminidase (NA) enzyme which is responsible for cleavage of sialic acids from the cell surface, to facilitate the spread of progeny virions. Influenza A is further divided into subtypes depending on the HA (18 subtypes) and NA (11 subtypes). Two influenza A subtypes are endemic in humans, (H1N1) and (H3N2). Zoonotic transmission may occasionally occur from birds and swine, including the highly pathogenic avian (H5N1) and (H7N9) viruses and the A(H1N1)pdm09 pandemic swine virus.

There are 9 residues in the NA active site which are highly conserved across all influenza A and B and which interact directly with substrate. These in turn are stabilized by a second shell of 10-11 highly conserved residues, primarily by an extensive network of hydrogen bonds.[1-4] These are defined as framework as they make no direct contact with the substrate but hold the functional residues in place for binding and catalysis.

There are now four drugs which target the NA, neuraminidase inhibitors (NAIs), which due to the high conservation of the NA active site are effective against all strains of influenza. Four NAIs are licensed in various parts of the world for the treatment and prevention of influenza, oseltamivir, zanamivir (**1**) (Figure 1), peramivir and laninamivir,[5] a long acting derivative of zanamivir. By inhibiting the influenza NA they prevent virus release, resulting in aggregation of viruses at the cell surface.[6] Because of differences in the chemistry of the NAIs and subtle differences in NA structures they can bind with a different affinity to the same subtype. e.g. oseltamivir has lower IC_{50}s than zanamivir for N2 NAs, whereas zanamivir has lower IC_{50}s than

oseltamivir for N1 and influenza B NAs[5, 7]. Additionally, due to these differences, resistance can

be both NAI and subtype specific.[5, 7] While mutations conferring resistance are primarily in

active site residues, mutations remote from the active site can also confer resistance.[5] Thus, in

developing novel NAIs they need to be evaluated against different influenza types and subtypes

and against different known resistant mutants of influenza.

We recently demonstrated that the difluorosialic acid (DFSA) mechanism based inhibitor 5-

(Acetylamino)-2,3,5-trideoxy-2,3-difluoro-D-erythro-β-L-manno-2-nonulopyranosonic acid **(2)**

(Figure 1) and its C-4 amino- and guanidino- derivatives, could inhibit the NA enzyme activity

and replication of influenza viruses both *in vitro* and *in vivo*.[8] We showed by X-ray

crystallography that **2** leads to inactivation of enzyme activity by the formation of a covalent

bond between the C-2 of the sugar ring and the hydroxyl group of Y406 in the influenza enzyme

active site. This covalently linked sialosyl-enzyme intermediate was trapped along with a

transition-state analogue resembling an oxocarbenium ion.[9] Also, the secondary non-catalytic,

receptor binding site was occupied by DFSA in the influenza N9 NA–DFSA complex.

In addition to the 4-amino and 4-guanidino derivatives of **2**, we have now synthesized a series of

deoxygenated DFSA derivatives **3**–**6** (Figure 1) in order to understand the contribution of each

hydroxyl in binding and inhibition of these sialic acid based inhibitors to the influenza NA.[10]

The influenza strains selected for evaluating the impact of removal of the OH groups were those

of clinical importance to humans, including the endemic human strains seasonal A(H1N1),

pandemic (H1N1)pdm09, A(H3N2) and B, and avian A(H5N1) and the A(H1N9) reassortant, as

a model for the avian A(H7N9) NA. NAI resistant mutants of some of these viruses, with

different resistance profiles, were also used in the enzyme assays. Some of these were previously

tested against other DFSA inhibitors[8] and interestingly not all mutants were resistant to the

DFSA inhibitors. Among the resistant viruses tested, the impacts of the amino acid substitutions on sensitivity to the known NAIs are as follows: D197E in influenza B NA affects binding of all sialic acid derived NAIs, due to altered interactions of the N-acetyl group on the ring with R152,[11] H274Y in N1 NAs affects rotation of E276 necessary for binding the pentyl ether side chain of oseltamivir[12] with only a small impact on binding of zanamivir, E119V in N2 NAs affects interactions of the 4-amino group on oseltamivir with the active site, E119G in N9 NAs specifically confers resistance to zanamivir, due to changes in the solvent structure and altered interactions of G119 with the 4-guanidino group.[13] An H252Y substitution between avian (H5N1) clade 1 and 2 viruses leads to reduced oseltamivir sensitivity.[14]

The NAIs oseltamivir and **1** are competitive inhibitors and a fluorescence based enzyme inhibition assay is routinely used for evaluating the sensitivity of influenza virus NAs *in vitro*.[7, 15-17] However, normally only a single IC_{50} value is calculated after 30-60 min.[7, 17] While a single IC_{50} value provides details on the relative affinity of these NAIs it does not provide any information on the relative rates of drug binding. As compound **1** is a competitive inhibitor, its efficacy is strongly reflected by its affinity (IC_{50}) for the NA. However, since compounds **2-6** are mechanism based inhibitors,[8] their efficacy is dependent not only on the affinity, but upon both the rate of inactivation, (dependent on both the Michaelis complex formation as well as the subsequent covalent bond formation), and the rate of reactivation (breakdown of the covalent intermediate followed by dissociation of the product). Kinetic analyses of inhibitor binding and dissociation requires large amounts of purified enzyme/virus and are labour intensive,[8, 18] limiting the numbers of virus/inhibitor combinations that can be readily assayed.

We have developed two microtiter fluorescence based enzyme inhibition assays which use unpurified virus, and instead of taking a single reading, monitor the reactions in real time. The

IC_{50} kinetics assay monitors the changes in IC_{50} values for each 10 min over 60 min, in two separate reactions with and without pre-incubation. This provides information on not only relative affinity (IC_{50}), but the relative rates of binding and dissociation of each of the compounds[16, 19] A solid phase reactivation assay monitors the time to recover activity after removal of inhibitor over several hours.[19] We have previously used these assays to demonstrate slow binding kinetics and rates of dissociation of the NAIs consistent with those observed using purified NA in the classic assays.[16, 19-22] Additionally, we have shown that while wild type viruses generally demonstrate slow binding of the known NAIs, the NAs of resistant mutants demonstrate rapid binding and dissociation of the NAIs.[11, 15, 16, 19, 23, 24]

We have used these assays here to compare relative inhibition of the NAs of a large panel of wild type and drug resistant mutants by each of the deoxy derivatives **3-6**. For the sake of simplicity, we will refer to inactivation as binding and reactivation as dissociation as we are also comparing them to the binding and dissociation of competitive NAIs.

In addition, we have evaluated the efficacy of **3-6** to inhibit replication of wild type viruses in cell culture in a plaque reduction assay. We show that loss of the 8- and 9-OH have the biggest impact on the affinity of binding and antiviral potency both *in vitro* and in cell culture.

We have also used structural analysis by X-ray crystallography of the N9 NA in complex with each of the inhibitors, to help explain the biological impact of the removal of the OH groups on binding. While we have used the G70C (H1N9) virus as a model virus and its NA for structural studies for many years, the N9 subtype has become more relevant due to the emergence of a highly lethal (H7N9) virus in China.[25, 26]

2. Results

2.1 IC$_{50}$ Kinetics

Compounds **1-6** were all evaluated in the microtiter based IC$_{50}$ kinetics assays against each of the

wild type and mutant viruses in the panel. IC$_{50}$ values for each time point were calculated as the

concentration of inhibitor which reduced the NA enzyme activity by 50% compared to the

control uninhibited enzyme activity. We used zanamivir as a reference for a slow binding

inhibitor with high affinity.[16] The greater the difference in final (60 min) IC$_{50}$ values between the

reactions without and with preincubation (-/+ ratio), the slower the binding (Figures 2 and 3,

Table 1). We have previously shown for the NAIs that fast binding inhibitors have a -/+ ratio of

around 1 for the 60 min IC$_{50}$ values, and slower binding inhibitors have ratios of >1.5-2,

indicating that preincubation enhances binding. Additionally, the rate of increase of the IC$_{50}$

values after preincubation with inhibitor upon addition of MUNANA substrate, gives a

qualitative indication of the dissociation rate. The faster the increase, i.e. the greater the

difference between the 10 min and 60 min IC$_{50}$ values, the faster the dissociation. A lower ratio

indicates slower dissociation (Figures 2 and 3, Supporting information Table S1). All assays

were carried out in duplicate as described in the Experimental section. The IC$_{50}$ value for each 10

min time point is the mean of the individual IC$_{50}$ values of the duplicates for that virus-inhibitor

reaction. The profiles of the bar graphs (Figures 2 and 3) provide an easy overview of changes in

IC$_{50}$ values for the large number of virus and compound combinations, showing whether the IC$_{50}$

values increase or decrease with and without preincubation over the 60 min reaction time,

indicative of fast or slow binding/dissociation. Comparisons of the 60 min IC$_{50}$ values without

and with preincubation, as an indication of relative slow or fast binding are all presented in Table

1. Comparisons of the change in IC$_{50}$ values between 10 and 60 min, as an indication of the

relative dissociation rate, are all presented in Supporting information, Table S1.

2.1.1 N1 NAs

The compounds were tested against the seasonal (H1N1) and H274Y oseltamivir resistant

viruses, swine and human isolates of (H1N1)pdm09 viruses, and two avian (H5N1) viruses,

which differ in oseltamivir sensitivity. None of the inhibitors showed the classic slow binding

profile of the bar graphs seen with zanamivir **(1)**, where the IC_{50} values continue to decrease

without preincubation from 10 to 60 min, and are significantly lower after preincubation (Figure

2, Table 1).

Despite large sequence differences between the (H1N1)pdm09 and (H5N1) NAs their kinetics

profiles were very similar for each of the inhibitors (Figures 2B, 2C), but both were different to

the seasonal (H1N1) NA and its H274Y mutant (Figure 2A). Consistent with previous findings,

clade 1 (H5N1) NA showed faster dissociation of **1** than clade 2 NA[16, 19] (Figure 2C and

Supporting information Table S1).

IC_{50} kinetics profiles for compounds **2** and **3** were similar to those previously seen with NAI

resistant mutant NAs.[16] They showed fast binding/dissociation to both the (H1N1)pdm09 and

(H5N1) NAs, with similar IC_{50} values with or without preincubation. In contrast, **2** demonstrated

slow binding to the seasonal (H1N1) NA, while the loss of 4-OH increased both the affinity and

rate of binding for compound **3** (Figure 2 and Table 1).

Removal of the 7-OH resulted in slightly higher affinity of **4** for the wild type seasonal (H1N1)

NA and slow binding. As seen with **2,** loss of the 7-OH resulted in reduced affinity to the H274Y

mutant NA. However, unlike previous mutant NAs, it had different binding kinetics. The IC_{50}

values were similar with or without preincubation, but continued to decrease in both reactions.

Rather than fast binding this indicated slower binding/dissociation (Figure 2A, Table 1,

Supporting information Table S2).

Loss of the 8-OH resulted in compound **5** binding with a much lower affinity to all the N1 NAs

compared to compounds **2**, **3** or **4**. Kinetics showed an unusual pattern of binding to the

(H1N1)pdm09 and clade 2 (H5N1) NAs, where the IC_{50} values were not significantly different

with or without preincubation, however they continued to decrease after the addition of substrate

(Figure 2B, C). We have not previously observed this with other NAIs binding to wild type NAs,

but it suggested there was slower turnover, possibly because of both slow binding and slow

dissociation. In contrast, there was an increase in IC_{50} values for the clade 1 (H5N1) NA after

preincubation with **5**, indicating a faster dissociation (Figure 2C, Supporting information Table

S1).

Loss of the 9-OH also had a significant impact on the affinity of the compounds, with a 1-2 log_{10}

increase in IC_{50} values for all the N1 NAs. There were larger differences in the IC_{50} values with

and without incubation for the seasonal (H1N1) and the H274Y mutant NAs with both **5** and **6**,

indicating slower binding compared to some of the other compounds. Except for the clade 1

(H5N1) NA the IC_{50} values continued to decrease with or without preincubation for these two

compounds. This suggested both **5** and **6** had a slow turnover.

2.1.2 N2 NA

IC_{50} kinetics for the H3N2 and oseltamivir resistant E119V NAs showed loss of the 4-OH

improved affinity (lower IC_{50} values) of **3** binding to the wild type H3N2 NA, compared to **2**

although it was still fast, with no significant effect of preincubation on IC_{50} values (Figure 3A,

Table 1). While **2** binds with higher affinity to the E119V mutant than to wild type, in contrast **3**

binds with lower affinity to the mutant NA.

9

Loss of the 7-OH improved affinity, with lower IC_{50} values for **4** than for **2** for both the wild type and E119V mutant NAs. As seen for **2,** compound **4** bound with higher affinity to the mutant NA, and it also showed slower binding than to the wild type NA.

While loss of either the 8-OH or 9-OH resulted in significantly reduced affinity, IC_{50} values were similar for each of the compounds for both the wild type and E119V mutant. Compound **5** showed the classic slow binding profile for both wild type and E119V NAs, with about a 10-fold decrease in IC_{50} values after preincubation, and slow dissociation, with a small increase in IC_{50} values with time after addition of substrate. Compound **6** showed the unusual profile, similar to the seasonal (H1N1), with the IC_{50} values continuing to decrease with or without preincubation (Figure 3, Table 1, Supporting information Table S1).

2.1.3 N9 NA

The G70C H1N9 reassortant was used to evaluate inhibition of the N9 NA, as a model for the N9 NA of the pathogenic (H7N9) viruses recently spreading in China.[25, 26] Compound **2** was fast binding to the wild type N9 NA. Although the IC_{50} values were comparable between the E119G mutant and wild type NAs (Figure 3B, Table 1 and Supporting information Table S2) the bar graph profiles showed the IC_{50} values decreased with or without preincubation for the E119G mutant NA, suggesting slower turnover. In contrast to **2**, compound **3** demonstrated higher affinity, but slower binding to the wild type N9 NA (Figure 3B, Table 1). While the E119G mutant showed the classic resistance profile of higher IC_{50} values, fast binding and dissociation, with IC_{50} values increasing with or without preincubation, as seen for this mutant with zanamivir[16] (Table 1, Supporting information Tables S1, S2), the loss of the 4-OH did not affect the affinity of binding to this mutant NA compared to **2**. It did however decrease binding of **3** compared to the wild type N9 NA (Supporting information Table S2).

Compared to **2**, loss of the 7-OH led to a higher affinity of **4** for the wild type N9 NA. In contrast, while **4** had reduced binding to the E119G NA compared to the wild type (Supporting information Table S2), loss of the 7-OH had no impact on binding to this mutant NA compared to **2**. (Supporting information Table S1).

Both **5** and **6** demonstrated a further decrease in IC_{50} values with or without preincubation over the 60 min reaction time, indicating slow turnover. As seen for all the other viruses the loss of either the 8-OH or the 9-OH reduced their affinity. The E119G substitution also reduced binding of both inhibitors, compared to the wild type NA and compared to **2** (Supporting information, Table S2). This reinforces the importance of both the 8- and 9-OH groups for high affinity binding. It further highlights the complex interactions involved in ligand binding, since the 8- and 9-OH groups are on the opposite side of the active site, compared to E/G119.

2.1.4 B NA

The B/Perth viruses were used to evaluate efficacy against wild type and broadly NAI resistant influenza B NAs. The D197E mutation results in reduced affinity and faster dissociation of **1** (Figure 3C, Table 1, Supporting information Table S1), and because the D197E substitution affects interaction of R152 with the N-acetyl group on the sugar ring, it would be expected to affect binding of all sialic acid based inhibitors.

Compared to **2**, loss of the 4-OH, as with the influenza A NAs, led to higher affinity of **3** (Figure 3C). Unexpectedly **3** bound with similar affinity to both the wild type and E197 mutant NA, somehow compensating for the reduced binding due to the altered E197/R152 interactions with the N-acetyl group (Figure 3C, Supporting information Table S2). Both showed the classic slow binding profile, with IC_{50} values after preincubation being lower than without preincubation (Figure 3C, Table 1).

Compounds **4, 5** and **6** all had reduced affinity (higher IC_{50} values) for the mutant NA compared

to the wild type NA, (Supporting information Table S2). However, unlike **1**, compounds **2-6** still

demonstrated slow binding to the B/Perth wild type and mutant NA (Table 1 and Supporting

information Table S1).

Loss of the 7-OH resulted in a marginally higher affinity compared to **2** (Table 1), but loss of the

8- or 9-OH groups again reduced affinity of **5** and **6** for both wild type and the D197E NAs,

while maintaining the slow binding, and slow dissociation seen with other viruses (Table 1,

Supporting information Table S1).

With the NAIs the ratio of -/+ preincubation has been a good indicator of slow and fast binding.

However, for compounds **5** and **6** the -/+ ratios in Table 1 clearly do not fully reflect what

appears to be slow turnover, since the IC_{50} values continue to decrease after preincubation

indicating additional compound is still binding. This demonstrates the importance of looking at

the profiles of the IC_{50} kinetics graphs, demonstrating the changes in IC_{50} values over time, rather

than a single IC_{50} value or -/+ ratio.

2.2. Reactivation

While our IC_{50} kinetics assays give an indication of the relative rate of dissociation after the

addition of substrate in the preincubation reaction (Supporting information Table S1), this is still

in the presence of inhibitor. The classic reactivation experiments react purified NAs or viruses

with excess inhibitor, then remove the unbound inhibitor by spin columns and monitor recovery

of enzyme activity after addition of substrate.[8, 18, 27-29] However this requires significant

quantities of virus or NA and is labor intensive. We had also seen a different pattern for the IC_{50}

kinetics especially for compounds **5** and **6** than previously seen with other NAIs binding to wild

type virus NAs, where although preincubation did not lead to obvious enhanced binding, the IC_{50}

values continued to decrease either with or without preincubation. We therefore used our 96-well

solid phase reactivation assay[19, 24] to test dissociation of **2-6** from the wild type virus NAs as a

further confirmatory assay to determine whether the novel profiles for **5** and **6** did reflect very

slow dissociation compared to **2-4**. The relative rate of reactivation is expressed as a T½ which is

the time required for reaching half the maximum average rate of the uninhibited control. Results

are shown in Table 2. The T½ results for each virus and inhibitor were compared to the T½ for

the virus controls without inhibitor, by the Student's t test. Consistent with the IC_{50} kinetics,

reactivation was significantly slower for compound **1** for all of the NAs (P <0.001).[19]

For the (H1N1) A/Mississippi seasonal strain, reactivation was significantly slower for **2-6**, with

6 being the slowest.

For the (H1N1)pdm09 and both (H5N1) strains, reactivation after removal of **2** and **3** was very

rapid, with T½ values barely more than 10 min. In fact, some ultimately showed an enhanced

rate of MUNANA cleavage compared to the control with no inhibitor. This is consistent with the

IC_{50} kinetics showing similar values with or without preincubation. Reactivation after removal of

3 was marginally faster than reactivation after removal of **4** for each of these viruses, but was not

significantly faster. Turnover of **5** and **6** were slower, as also seen in the IC_{50} kinetics, although

only significantly slower for the (H1N1)pdm09 and (H5N1) clade 2 viruses.

For the H3N2 NA, in contrast to compound **1**, reactivation after removal of compounds **3** and **4**

was very fast, comparable to the control. Reactivation after removal of compound **2** was just

significantly slower than the control. Turnover of **5** and **6** were significantly slower, again

consistent with the IC_{50} kinetics showing decreases in IC_{50} values in both reactions.

For the NWS/G70C N9 NA reactivation was very rapid after removal of compounds **2, 3** and **4** while reactivation after removal of **5** and **6** was significantly slower reflecting the results in the IC_{50} kinetics where the $IC_{50}s$ continued to decrease in the preincubation reaction. Reactivation of the B/Perth NA activity after removal of the inhibitors was slowest of all of the inhibitors **2-6,** even slower than for **1**. Results were consistent with the IC_{50} kinetics, with **3** having the fastest turnover of all the deoxy inhibitors for B/Perth, and **5** and **6** having the slowest turnover of any virus NA-DFSA combination.

2.3. Plaque reduction assay (PRA)

We have demonstrated in enzyme assays that while the loss of the 4-OH generally leads to lower affinity, it results in faster turnover. In contrast loss of the 8- and 9-OH groups result in lower affinity, but slower turnover. Since the ability of the covalent DFSA inhibitors to inhibit virus replication will be a combination of the relative affinity as well as their turnover we tested their efficacy against a selection of the wild type viruses in the PRA to see whether there was greater correlation with the slow turnover of affinity. The EC_{50} is the effective concentration of inhibitor to reduce plaque sizes by 50% compared to the uninhibited control. We tested the A/Mississippi/03/01 seasonal (H1N1) virus, the G70C H1N9 reassortant, the B/Perth/211/2001 virus and two different human H3N2 viruses, A/Fukui/45/04 and A/Victoria/503/06, as some H3N2 are known to have lower sensitivity to the other NAIs in cell culture, due to lower affinity of their HA. This lowers their dependence on the NA, making them appear less sensitive in a PRA, due to the altered HA and NA balance.

Inhibition of the (H1N1) A/Mississippi virus was comparable for compounds **2, 3** and **4** in the PRA (Table 3, Supporting information Figure S1). Despite very slow dissociation of **5** its

efficacy was less than that of the other inhibitors, and **6** was the least potent, reflecting the relative IC_{50} values in the enzyme inhibition assays.

All inhibitors, including **1** showed lower potency against the H3N2 A/Fukui/45/04 (Table 3) virus in the PRA compared to the other viruses. This is likely due to the HA having a lower affinity for the sialic acid receptor, hence less NA activity is needed for virus to elute and spread.[30] Although the IC_{50} values in the enzyme assay were lower for compounds **3** and **4** compared to compound **2**, there was no difference detectable in their potency in the PRA. Inhibition by **5** was even poorer, reflecting its lower efficacy in the enzyme assay, as we saw no inhibition even at 100 µM in the PRA.

Since the A/Victoria/503/06 H3N2 virus was more sensitive to zanamivir in the PRA, we also tested this virus with the DFSA panel. Both **3** and **4** showed higher potency compared to DFSA **2**, with lower efficacy of **5** and **6** (Table 3). This is consistent with the enzyme assay results seen with the A/Fukui/45/04 N2 NA.

All the inhibitors were mostly more potent against the B/Perth virus in the PRA than against the other influenza A viruses tested (Table 3), which was also observed in the IC_{50} kinetics assays. Once again, although **2, 3** and **4** had faster turnover compared to **5** and **6**, they were more potent than **5** and **6** with their slower turnover.

Thus, it appears that efficacy of inhibition of virus replication in cell culture primarily reflects the affinity of the compound for the NA, rather than the turnover rate.

2.4. X-ray crystal structures

2.4.1 Trapped intermediates in the active site

As seen previously with DFSA, **2**[9] binding of the deoxy compounds **3-6** resulted in the trapping of intermediates in the N9 NA. There is a clear rotation of the COOH group and loss of the fluorine (F2) at the C2 positon of the ligand. The ligands were trapped in the form of the two n-deoxy (n=4,7,8,9) 3-fluorosialyl-enzyme intermediates bound in the active site (Figure 4). A covalent bond of ~1.4 Å was observed in the electron density map between C2 of n-deoxy (n=4,7,8,9) 3-fluoro sialic acid and the phenolic oxygen of Y406 (Figure 4) consistent with previous results recently reported.[8] A covalent bond has also been observed previously in the structures of the bacterial GH33 sialidase NanI[31], N2 NA with a DFSA[32] and N9 NA with a DFSA derivative 3-equatorial-2,3-difluoro-4-guanidino sialic acid (FeqGuDFSA).[8]

Again, similar to the **2**-NA N9 complex[9] in addition to the covalent intermediate species detected, we also identified non-bonded species which we assumed to be unsaturated forms of n-deoxy 3-fluoro sialic acid intermediates with fractional occupancies: 20% / 80% (**3**), 45% / 55% (**4**), 60% / 40% (**5**), and 25% / 75% (**6**), respectively for covalently bonded and non-bonded species, (Figure 4A, C, E, G).

The distances between the anomeric C2 of non-bonded forms and the phenolic oxygen of Y406 are ~2.5 Å, much longer than the corresponding C-O covalent bond lengths observed for the covalent intermediates. This non-bonded form of the -n-deoxy fluorosialic acid intermediates is consistent with an oxocarbenium ion like transition state in which the carboxylate group is coplanar with the oxocarbenium ion plane with considerable sp^2 hybridization at the anomeric carbon. The oxocarbenium ion positive charge at the ring oxygen O6 is stabilized by hydrogen bonds with waters at 2.7-3.4 Å in all N9 complexes. The oxocarbenium ion is thus sandwiched between the active site negatively charged residues, in particular the deprotonated tyrosine and waters. Further, the oxocarbenium ion is also stabilized by electrostatic interactions with the

negatively charged carboxylate group adjacent to the anomeric carbon C2 and the fluorine

attached to the C3 carbon. These anionic charges assist with the departure of the negatively

charged fluorine leaving group and the formation of a covalent intermediate bound to the

phenolic oxygen of tyrosine. Because the oxocarbenium ion has double-bond character between

the anomeric carbon C2 and the ring oxygen O6, this part of the structure must be planar. Thus,

for a 6-membered ring, C2, O6, C1 and C3 must lie in a plane. This arrangement can be

accommodated in a 6-membered ring only in the half chair conformation similar to a glycal

DANA generated at a low rate from sialic acid soaked in crystals of the influenza B virus NA at

4°C for an extended time.[33] Similarly, the n-deoxy-DFSA fluorinated substrate analogues

facilitated trapping enzyme bound species resembling intermediates or "transition states". The

structures of assumed bonded and non-bonded ligands were refined from the observed

experimental electron density with stereochemical constraints. The ligands are stabilized by an

extended hydrogen bond network involving residues and structured water molecules, most of

them are well documented in the NA structures with sialic acid[1] and FeqGuDFSA.[8] In addition,

the fluorines make contacts in the range of 3.0-3.9 Å with the side chain nitrogen atom of R118

as well as short contacts in the range of 2.5-3.5 **Å** with the carboxyl oxygen of D151. Interactions

between fluorine and a protonated nitrogen are well known and have been computed at up to

13.5 kcal/mol.[8]

2.4.2 Ligands in additional receptor binding sites

The omit[34] electron density (Figure 4B, D, F, H) revealed one additional n-deoxy-DFSA

(n=4,7,8,9) site formed by three serines: **S367, S370** and **S372** (N2 numbering used throughout).

This is the known second site in the N9 NA, previously reported to bind sialic acid, which is

discrete from the catalytic site.[35] The n-deoxy-DFSA position is overlapping well with that for **2**[9]

and sialic acid in this second binding site[35] confirming that the secondary ligand sites in N9 NA

are not specific to the sialic acid complex only.

2.4.3 Compound 3

The secondary receptor binding site confirms the original structure of **3 (Figure 4B)**, prior to

binding and cleavage. According to kinetic assays above **3** binds with higher affinity than **2** to

the wild type N9 (Figure 3, Table 1). While the N9 E119G mutant NA has reduced binding of **3**

compared to the wild type, binding is similar to **2**, but shows a different kinetics profile

suggesting a faster turnover (Figure 3). E119 must provide important interactions, which are lost

with G119. This is most likely contacts of ~3 Å between the carboxyl groups of E119 and D151

and the F3 fluorines (Figure 4A). In the case of the wild type N9, the negatively charged 4-OH

group next to the electronegative F3 seems to destabilize the F3 contacts with E119 and D151

and the loss of 4-OH improves binding of **3**.

2.4.4 Compound 4

The crystal structure shows the second site (Figure 4D), again confirming the original **4** structure

prior to cleavage. The 7-OH group was mainly involved in contacts of ~2.5 Å with two waters as

seen in **2**[9] and **3** complexes (Figure4A). Loss of the 7-OH with those water contacts (Figure 4C)

would be expected to lead to minor changes in affinity to both the wild N9 and its E119G

mutant. In fact, **4** binds with slightly higher affinity to the wild type than **2**, and loss of the 7-OH

has no impact on binding to the mutant G119 NA compared to **2**.

2.4.5 Compound 5

In contrast to **3** and **4** N9 complexes, which were obtained by a short soak in ligands, we could

only obtain complexes for **5** and **6** by co-crystallization. The secondary ligand site in the co-

crystallized **5**-N9 complex showed fragmented electron density (Figure 4F), suggesting

18

fractional population of this site and reduced binding affinity. Also, in the active site (Figure 4E), 8-OH forms important contacts of 2.5-3.5 Å with COOH groups of E276 and E277, of 3.6 Å with R292 and of ~3Å with a water. Due to loss of the 8-OH there is an upwards displacement of the sugar ring of the ligand to the Y406, but there is also some rotation of both the E276 and E277 compared to other complexes.

2.4.6 Compound 6

Similar to **5**, the complex with **6** was only obtained by co-crystallization and showed high atomic displacement parameters and fragmented electron density for **6** in the secondary ligand binding site (Figure 4H). This again suggests slower binding and reduced affinity as seen for **5**. The active site shows (Figure 4G) loss of contacts between 9-OH and E276 (2.5 Å), R224 (3.3 Å), and a water (2.8 Å). Loss of these important contacts would correlate with the reduced binding affinity of **5** and **6** to not only the N9 but to all other NAs tested.

3. Discussion

Zanamivir (**1**) is reported to be a competitive, slow binding inhibitor of the influenza NAs. It has been suggested that the 4-guanidino side chain in **1** needs to displace water for high affinity binding, hence leading to slow binding.[20, 36] Without a guanidino substitution at the 4-position, as in 2-deoxy-2,3-didehydro-N-acetylneuraminic acid (DANA) and the 4-amino derivatives of sialic acid, binding to the NA is rapid.[16] Binding of **2** to influenza NAs would thus be expected to be rapid. The aim with a covalent inhibitor is to have high affinity binding, but additionally a slower turnover, since unlike competitive inhibitors, once a covalent inhibitor is hydrolyzed it cannot inhibit another NA.[8] We were interested in testing the impact of removal of one of each of the 4, 7-. 8- or 9-OH from **2** on binding affinity (inactivation), and dissociation/turnover

(reactivation) with a variety of different wild type and mutant N1, N2, N9 and influenza B NAs. Insight into the roles of each of the OH groups could provide important information on potential sites for substitution to enhance potency of the DFSA inhibitors, as well as understanding how ligand modifications affect binding to known NAI resistant mutants.

Our previous development of microtiter based assays has enabled us to test a large number of combinations of inhibitors and wild type and mutant viruses for their relative potency and kinetics of binding and dissociation in enzyme assays.[11, 15, 16, 19, 23, 24, 37] We observed much more variation in affinity and binding kinetics of **2** and **3-6** among different wild type viruses compared to **1**, oseltamivir and peramivir.[16] We showed here that while binding of **2** and some of the deoxy derivatives did not show the classic profile of slow binding inhibitors in the IC_{50} kinetics reaction to all the tested influenza A NAs, some also did demonstrate slow binding. Unexpectedly they all showed slow binding to not only the influenza B wild type NA, but also to the mutant influenza B NA. Additionally, in contrast to other NAIs where potency against influenza B is generally lower than to influenza A NAs, **2** and its deoxygenated derivatives **3-6** generally bound with higher affinity to the B/Perth NA, compared to influenza A NAs. This is consistent with our previous observations that **2** and its 4-amino and 4-guanidino derivatives bound with high affinity to influenza B NA.[8]

We have previously shown that mutations which confer reduced susceptibility to the NAIs , result in loss of slow binding, so that preincubation makes no difference,[11, 15, 16, 37] and inhibitors dissociate rapidly.[19] However while some of the deoxy DFSA inhibitors did show slow binding, and they had reduced affinity for mutant NAs compared to their wild type parent, many still showed either slow binding or slow turnover in the mutant NAs. Some of the mutant NAs even

bound the compound with higher affinity compared to the wild type NA. Thus, the mutations had minimal impact on binding **3-6**, compared to **2**.

In general, the loss of the 4-OH resulted in higher affinity binding (lower IC_{50} values) compared to **2** for wild type NAs, while the loss of the 8- and 9-OH resulted in lower affinity, but slower binding and turnover. We have previously determined that if the IC_{50} after preincubation (+) is lower than without preincubation (-), then the inhibitor is slow binding (-/+ ratio >1.5-2). However, here we observed a novel profile in the IC_{50} kinetics particularly for **5** and **6**, where with or without preincubation the IC_{50} values continued to decrease during the 60 min reaction time. This suggested a nett slower binding and dissociation, hence a slower turnover, which was not necessarily reflected by the -/+ ratio. This emphasizes the importance of looking at the graphs for the whole reaction time and not just a single IC_{50}. This interpretation was supported by the results of our reactivation assays, which demonstrated a slower reactivation than for the other compounds. We have only observed this unusual pattern of binding with **1** binding to an NAI resistant seasonal (H1N1) with a novel Y155H mutation.[15]

Additionally, we evaluated the inhibitors in a plaque reduction assay in cell culture, providing information on the nett effect of affinity and turnover on inhibition of virus replication and the importance of each OH group. While theoretically the inhibitor with the slowest turnover might be expected to have the highest nett potency in terms of inhibition of virus replication *in vivo*, this was not the case. Potency was more a reflection of the relative affinity, rather than the turnover. Both **5** and **6** which had the slowest turnover of all the compounds, had both the lowest affinity and the lowest potency. Conversely, **3** which had a rapid turnover, but higher affinity, was more potent than **5** and **6**. Thus, our studies have importantly demonstrated that slowing down turnover of these mechanism based inhibitors will not necessarily result in higher potency.

Structural analysis also supported the observed variation in ligand binding, showing the importance of water molecules in stabilizing ligands in the active site as well as the interactions of the 8-OH and 9-OH with E276/E277/R224/R292. X-ray crystallography demonstrated that like **2**[9] compounds **3-6** could also bind in the second sialic acid binding site.[35] This is a non-catalytic site and the biological role of this site is yet not understood. The NAIs do not bind this site, since they have a DANA boat-like conformation. Only ligands with the sialic acid chair conformation can bind, in a similar way to binding to the HA.[9] One study has shown that the ability of NA to bind red blood cells via this second site correlated with the cleavage efficiencies of other multivalent substrates.[38] Others have more recently shown that substrate binding via the second sialic acid-binding site in (H7N9) viruses enhances NA catalytic efficiency against the same substrate.[39] Hence binding in this site may affect affinity of the DFSA inhibitors, but not the kinetics. Thus an inhibitor which can bind both in the secondary sialic acid binding site as well as the NA active site, might have advantages in reducing virus binding and spread, particularly for avian viruses which continue to pose a pandemic threat.

4. Conclusions

Although the efficacy of covalent inhibitors is dependent on both the affinity and turnover, we have shown here that with the deoxy-DFSA inhibitors **3-6**, the advantages of a slower turnover can be counteracted by lower affinity. Hence the design of covalent inhibitors needs to incorporate modifications leading to both high affinity and slow turnover. Loss of the 8-OH and 9-OH had the greatest impact on binding and affinity of the covalent inhibitors tested here.

Experimental Section

Materials

Zanamivir **1** was kindly provided by GSK (Stevenage, UK) and compound **2** was kindly

provided by the group of Prof. Steve Withers (Vancouver, BC). Compounds **3-6** were prepared

as previously described.[10] The purity of final compounds was ≥95%. Purity was determined by

elemental analysis and is available in the Supporting Information.

Viruses and cells

The following wild type and drug resistant viruses were grown in cell culture as previously

described.[8, 16]: B/Perth/211/2001 wild type and D197E cross-resistant mutant,[40]

A/Mississippi/03/01 seasonal (H1N1) and H274Y oseltamivir and peramivir resistant mutant,[7]

A/Fukui/45/04 H3N2 wild type and E119V oseltamivir resistant mutant,[17] A/Victoria/503/06

H3N2 grown in MDCK cells,[41] NWS/G70C H1N9 and E119G zanamivir and peramivir resistant

mutant.[13, 42] The following irradiated viruses were provided by the CSIRO Australian Animal

Health Laboratory for enzyme assays only (H1N1)pdm09 A/California/7/09 and

A/Swine/Shepparton/6/2009, and A/Chicken//Vietnam/08/2004 (H5N1) clade 1and

A/Chicken/Bangli/BBVD-563/2007clade 2 (H5N1).[37]

Plaque reduction assays (PRAs) in Madin Darby Canine Kidney cells (MDCK) were carried out

as previously described[8, 23] using an overlay of DMEM/ F12 in 0.5% immunodiffusion-grade

agarose (MP Biomedicals, Australia), containing 1 mg/mL L-1-tosylamido-2-phenylethyl

chloromethyl ketone ('TPCK')-treated trypsin (Worthington, USA). Serial ten-fold dilutions of

inhibitors were incorporated into the overlay[23] and cells were fixed at 3 days with 1% formalin,

and stained with 0.05% neutral red and scanned. The EC_{50} is the effective inhibitor concentration

causing a 50% decrease in plaque size. Where there was greater than 50% reduction in plaque size between two drug concentrations a range was used.

Enzyme assays

NA enzyme activity was measured using the fluorescent substrate 4-Methylumbelliferyl N-acetyl-α-D-neuraminic acid (MUNANA, Carbosynth, Berkshire, UK). MUNANA was diluted to a final concentration of 100 µM in 50 mM sodium acetate pH 5.5 and 5 mM $CaCl_2$. We used a BMG FLUOstar Optima reader and the kinetics function for real time monitoring of the fluorescent signals. Fluorescence was read using excitation and emission filters 355 and 460 nm respectively.

All viruses were initially titrated to determine a dilution which gave similar NA enzyme activity. Inhibition assays were carried out using the constant amount of each virus, incubated with seven serial 10-fold dilutions of each inhibitor. Inhibitor concentrations ranged from 0.01 nM to 10 mM depending on the compound, with the lowest range for compound **1** only. The eighth well contained virus only as the uninhibited control. Graphs of concentration of inhibitor versus % inhibition of enzyme activity compared to the uninhibited control were plotted in Sigmaplot. The IC_{50} values were determined as the concentration of inhibitor which reduced the enzyme activity by 50% compared to the control.

While the IC_{50} for NAIs is routinely calculated for a single time point after the addition of MUNANA, (usually 60 min), because the NAs are described as time dependent, or slow binding inhibitors,[20, 21] we have previously shown that the IC_{50} changes during the reaction time, and is dependent upon whether the virus is preincubated with inhibitor, or not.[11, 16, 23] Based on this observation we developed an IC_{50} kinetics enzyme inhibition [11, 16, 23] assay which has provided

information on the relative rates of inhibitor binding, and the relative rates of dissociation of

many different wild type and mutant viruses and NAIs.[11, 15, 16, 23, 24, 37] For IC_{50} kinetics two

separate inhibition assays were carried out. In the first reaction virus was preincubated with

serial 10-fold dilutions of inhibitor for 30 min at room temperature, prior to the addition of

substrate, and in the second reaction virus, serial 10-fold dilutions of inhibitor and MUNANA

substrate were all co-incubated. Fluorescence was read every minute for 60 min and the percent

inhibition of enzyme activity for each 10 min time point compared to the uninhibited control was

plotted against the concentration of inhibitor. The IC_{50} values were determined for each 10 min,

hence 6 inhibition curves and 6 IC_{50} values were calculated for each reaction. Each virus-

inhibitor combination was tested in duplicate for each of the pre incubation and no preincubation

reactions. IC_{50} values were calculated independently for each 10 min time point for each of the

duplicates and the mean IC_{50} values were then plotted as bar graphs to demonstrate the changes

in IC_{50} with time i.e. the IC_{50} kinetics.

Solid phase reactivation assays were carried out as recently described.[19, 24] Briefly, after binding

virus to multiple wells in a black ELISA plate (Greiner Fluorotrack 600), inhibitor was added at

>10 times the IC_{50} and incubated for 30 min. Inhibitor was then washed off, MUNANA substrate

was added, and the reactivation of enzyme activity was monitored after each 10 min for 4 hours.

The relative rates of activity were calculated compared to the uninhibited virus control for each

30 min period, and if reactivation was rapid, rates for the initial 10 and 20 min were calculated.

The T½ was calculated as the time taken for the rate to reach half the maximum rate of the

control.[19] Two or three wells for each drug were used per assay in two independent assays.

Statistics

Data for reactivation assays were analyzed for statistical significance using a Student's *t* test, where a *P* value of <0.05 was considered statistically significant.

Crystallization

NA from influenza virus A/NWS/Tern/Australia/G70C/75 was purified as described previously[13] and crystallized in potassium phosphate buffer (1.7 M, pH 6.7) as previously described.[35] The N9-NA **3** and **4** complexes were prepared by soaking crystals in cryo-protectant solution containing crystallization well solution plus 20% glycerol and 2 mM concentration of inhibitor for 30 min at ambient temperature and 15 min at 4°C, respectively. The N9-NA **5** and **6** complexes were prepared by co-crystallization.

X-ray data collection, structure determination, and refinement

X-ray diffraction data sets for single crystals of N9 NA with inhibitor complexes in well solution plus 15% (v/v) glycerol as cryo-protectant were collected at -173°C with 360° rotation, 1o oscillation and 1s exposure with wavelength of ~0.95 Å using the MX1/MX2 beamlines at the Australian synchrotron. The data sets were processed with HKL2000.[43] Further data collection statistics are given in Table 4. The positions of one N9 NA molecule were identified in the asymmetric units by PHASER [44] molecular replacement using the structure of N9 (PDB entry: 1NNC)[35] without ligands. The structures with protein molecules alone were refined and then the inhibitors were built into the observed residual electron densities.

Initial refinement of the inhibitor position did not account for all the residual density observed in all N9 NA protein structures. In particular, there was slight negative residual density around the F3 atom and positive residual density in the region between the inhibitor and the Y406 (N9 NA)

residue. The continuous bridge of residual electron density between the C2 atom of the inhibitor and hydroxyl oxygen of the aromatic side chain of Y406 residue suggested the C-O covalent bond, however the refined bond distance was always longer than the expected covalent bond of ~1.4Å. Next, the covalent intermediate species accompanied by unsaturated forms of fluorosialic acid as oxocarbenium ion transition-state analogues were refined in N9 NA protein structures. The geometry of unsaturated forms of fluorosialic acid species is similar to that of DANA in which the carboxylate group is coplanar with the ring plane with considerable sp2 hybridization at the anomeric carbon. Since a fluorine atom is refined at the chiral position, the double bond is between the ring oxygen and the anomeric carbon, with positive charge at the oxygen resembling an oxocarbenium ion transition state. Adjusting the occupancies of two bonded and non-bonded conformations the length of the covalent linkage for bonded species was refined to a chemically sensible value of ~1.4 Å. After that the corresponding LINK record was added to the PDB files to define this bond. The occupancies of two conformations were refined to 20% / 80% (**3**), 45% / 55% (**4**), 60% / 40% (**5**), and 25% / 75% (**6**) respectively for covalently bonded and non-bonded species. The refinement of occupancy was carried iteratively alternating fixed B-factors or occupancies until physically meaningful and similar for both species values of atomic B-factors were obtained.

In addition, the secondary binding site for molecules of all deoxy-DFSA were identified in the N9 NA complexes, by difference Fourier methods during the course of the refinement. It should be noted that both soaking and co-crystallization were sufficient to observe the initial binding events of **2** including secondary sites and a variable mixed occupancy of the active site. Electron densities for secondary sites of co-crystallized complexes of **5** and **6** were less defined and somewhat fragmented.

Water molecules in the active site and elsewhere were then added. Iterative refinement and model building were conducted using REFMAC[45] and XFIT/MIFit.[46, 47] N-linked glycans were observed at all predicted sites (N86, N146 and N201) and are included in the refined atomic model. Refinement yielded a model for 388 residues for the N9 with 11 attached glycans, 1 calcium ion, two alternating conformations of the inhibitor, 1 n-deoxy DFSA molecule at additional site and 430 (**3**), 423 (**4**), 483 (**5**), and 354 (**6**) water molecules (Table 4). Progress of the refinement was monitored using the Rfree statistics based on a test set encompassing 5% of the observed diffraction amplitudes.[48] The coordinates of the complexes have been deposited in the PDB. Deposition codes and further experimental and data processing details are given in Table 4. Final omit electron densities associated with the ligands in active site and secondary binding sites are displayed in Figure 4 for all N9 NA – inhibitor complexes.

ASSOCIATED CONTENT

Supporting Information

The Supporting Information is available free of charge on the ACS Publications website at DOI:

Comparison of IC_{50} values for 10 and 60 min in the preincubation reaction **(Table S1)**,

Fold difference between wild type and mutant 60 min IC_{50} values in the preincubation

reaction **(Table S2)**.

Plaque reduction assay for seasonal influenza (H1N1) A/Mississippi/03/01 **(Figure S1)**,

Molecular formula strings **(PDF)**

Molecular formula strings **(CSV)**

Accession Codes

Crystal structures of influenza neuraminidase N9 in complex with compounds **3** (PDB 5W26), **4**

(PDB 5W2U), **5** (PDB 5W2W), and **6** (PDB 5W2Y). Authors will release the atomic

coordinates and experimental data upon article publication.

Corresponding author Jennifer L McKimm-Breschkin

+61 3 8344 1106

jmbvirology@gmail.com

Current addresses

Jennifer L McKimm-Breschkin

Department of Microbiology and Immunology, University of Melbourne, Peter Doherty Institute,

Melbourne, 3000 Australia

Stefan Hader

Kings College London, Strand, London, WC2R 2LS, UK Stefan.hader@kcl.ac.uk

Author contributions

JMB analysed data, prepared NA for crystallisation, wrote the manuscript, SB carried out IC_{50} kinetics, reactivation assays and plaque assays, SH synthesized the compounds, AW wrote the manuscript, supervised synthesis of the compounds, PP crystallized the NA, VS did the X-ray crystallography and structural analysis and wrote the manuscript.

Abbreviations: NA neuraminidase, NAI neuraminidase inhibitor, DFSA difluoro sialic acid,

Conflict of Interest

The authors declare no competing financial interest

References

(1)   Varghese, J. N.; McKimm-Breschkin, J. L.; Caldwell, J. B.; Kortt, A. A.; Colman, P. M. The structure of the complex between influenza virus neuraminidase and sialic acid, the viral receptor. *Proteins* **1992,** *14*, 327-332.

(2)   Burmeister, W. P.; Ruigrok, R. W.; Cusack, S. The 2.2 A resolution crystal structure of influenza B neuraminidase and its complex with sialic acid. *EMBO J.* **1992,** *11*, 49-56.

(3)   Varghese, J. N.; Colman, P. M. Three-dimensional structure of the neuraminidase of influenza virus A/Tokyo/3/67 at 2.2 A resolution. *J. Mol. Biol.* **1991,** *221*, 473-486.

(4)   Colman, P. M.; Hoyne, P. A.; Lawrence, M. C. Sequence and structure alignment of paramyxovirus hemagglutinin-neuraminidase with influenza virus neuraminidase. *J. Virol.* **1993,** *67*, 2972-2980.

(5)   McKimm-Breschkin, J. L. Influenza neuraminidase inhibitors: antiviral action and mechanisms of resistance. *Influenza Other Respir Viruses* **2013,** *7 Suppl 1*, 25-36.

(6)   Tarbet, E. B.; Hamilton, S.; Vollmer, A. H.; Luttick, A.; Ng, W. C.; Pryor, M.; Hurst, B. L.; Crawford, S.; Smee, D. F.; Tucker, S. P. A zanamivir dimer with prophylactic and enhanced therapeutic activity against influenza viruses. *J. Antimicrob. Chemother.* **2014,** *69*, 2164-2174.

(7)   Monto, A. S.; McKimm-Breschkin, J. L.; Macken, C.; Hampson, A. W.; Hay, A.; Klimov, A.; Tashiro, M.; Webster, R. G.; Aymard, M.; Hayden, F. G.; Zambon, M. Detection of influenza viruses resistant to neuraminidase inhibitors in global surveillance during the first 3 years of their use. *Antimicrob. Agents Chemother.* **2006,** *50*, 2395-2402.

(8)   Kim, J. H.; Resende, R.; Wennekes, T.; Chen, H. M.; Bance, N.; Buchini, S.; Watts, A. G.; Pilling, P.; Streltsov, V. A.; Petric, M.; Liggins, R.; Barrett, S.; McKimm-Breschkin, J. L.;

Niikura, M.; Withers, S. G. Mechanism-based covalent neuraminidase inhibitors with broad-spectrum influenza antiviral activity. *Science* **2013,** *340*, 71-75.

(9)   Streltsov, V. A.; Pilling, P.; Barrett, S.; McKimm-Breschkin, J. L. Catalytic mechanism and novel receptor binding sites of human parainfluenza virus type 3 hemagglutinin-neuraminidase (hPIV3 HN). *Antiviral Res.* **2015,** *123*, 216-223.

(10)   Hader, S.; Watts, A. G. The synthesis of a series of deoxygenated 2,3-difluoro-N-acteylneuraminic acid derivatives as potential sialidase inhibitors. *Carbohydr. Res.* **2013,** *374*, 23-28.

(11)   Oakley, A. J.; Barrett, S.; Peat, T. S.; Newman, J.; Streltsov, V. A.; Waddington, L.; Saito, T.; Tashiro, M.; McKimm-Breschkin, J. L. Structural and functional basis of resistance to neuraminidase inhibitors of influenza B viruses. *J. Med. Chem.* **2010,** *53*, 6421-6431.

(12)   Collins, P. J.; Haire, L. F.; Lin, Y. P.; Liu, J.; Russell, R. J.; Walker, P. A.; Skehel, J. J.; Martin, S. R.; Hay, A. J.; Gamblin, S. J. Crystal structures of oseltamivir-resistant influenza virus neuraminidase mutants. *Nature* **2008,** *453*, 1258-1261.

(13)   Blick, T. J.; Tiong, T.; Sahasrabudhe, A.; Varghese, J. N.; Colman, P. M.; Hart, G. J.; Bethell, R. C.; McKimm-Breschkin, J. L. Generation and characterization of an influenza virus neuraminidase variant with decreased sensitivity to the neuraminidase-specific inhibitor 4-guanidino-Neu5Ac2en. *Virology* **1995,** *214*, 475-484.

(14)   McKimm-Breschkin, J. L.; Selleck, P. W.; Usman, T. B.; Johnson, M. A. Reduced sensitivity of influenza A (H5N1) to oseltamivir. *Emerg. Infect. Dis.* **2007,** *13*, 1354-1357.

(15)   McKimm-Breschkin, J. L.; Williams, J.; Barrett, S.; Jachno, K.; McDonald, M.; Mohr, P. G.; Saito, T.; Tashiro, M. Reduced susceptibility to all neuraminidase inhibitors of influenza

H1N1 viruses with haemagglutinin mutations and mutations in non-conserved residues of the neuraminidase. *J. Antimicrob. Chemother.* **2013,** *68*, 2210-2221.

(16)   Barrett, S.; Mohr, P. G.; Schmidt, P. M.; McKimm-Breschkin, J. L. Real time enzyme inhibition assays provide insights into differences in binding of neuraminidase inhibitors to wild type and mutant influenza viruses. *PLoS One* **2011,** *6*, e23627.

(17)   Tashiro, M.; McKimm-Breschkin, J. L.; Saito, T.; Klimov, A.; Macken, C.; Zambon, M.; Hayden, F. G. Surveillance for neuraminidase-inhibitor-resistant influenza viruses in Japan, 1996-2007. *Antivir. Ther.* **2009,** *14*, 751-761.

(18)   Watts, A. G.; Oppezzo, P.; Withers, S. G.; Alzari, P. M.; Buschiazzo, A. Structural and kinetic analysis of two covalent sialosyl-enzyme intermediates on Trypanosoma rangeli sialidase. *J. Biol. Chem.* **2006,** *281*, 4149-4155.

(19)   Barrett, S.; McKimm-Breschkin, J. L. Solid phase assay for comparing reactivation rates of neuraminidases of influenza wild type and resistant mutants after inhibitor removal. *Antiviral Res.* **2014,** *108*, 30-35.

(20)   Pegg, M. S.; von Itzstein, M. Slow-binding inhibition of sialidase from influenza virus. *Biochem. Mol. Biol. Int.* **1994,** *32*, 851-858.

(21)   Kati, W. M.; Saldivar, A. S.; Mohamadi, F.; Sham, H. L.; Laver, W. G.; Kohlbrenner, W. E. GS4071 is a slow-binding inhibitor of influenza neuraminidase from both A and B strains. *Biochem. Biophys. Res. Commun.* **1998,** *244*, 408-413.

(22)   Baum, E. Z.; Wagaman, P. C.; Ly, L.; Turchi, I.; Le, J.; Bucher, D.; Bush, K. A point mutation in influenza B neuraminidase confers resistance to peramivir and loss of slow binding. *Antiviral Res.* **2003,** *59*, 13-22.

(23)   McKimm-Breschkin, J. L.; Rootes, C.; Mohr, P. G.; Barrett, S.; Streltsov, V. A. In vitro

passaging of a pandemic H1N1/09 virus selects for viruses with neuraminidase mutations

conferring high-level resistance to oseltamivir and peramivir, but not to zanamivir. *J.*

Antimicrob. Chemother. **2012,** *67,* 1874-1883.

(24)   McKimm-Breschkin, J. L.; Barrett, S. Neuraminidase mutations conferring resistance to

laninamivir lead to faster drug binding and dissociation. *Antiviral Res.* **2015,** *114*, 62-66.

(25)   Zhou, J.; Wang, D.; Gao, R.; Zhao, B.; Song, J.; Qi, X.; Zhang, Y.; Shi, Y.; Yang, L.;

Zhu, W.; Bai, T.; Qin, K.; Lan, Y.; Zou, S.; Guo, J.; Dong, J.; Dong, L.; Wei, H.; Li, X.; Lu, J.;

Liu, L.; Zhao, X.; Huang, W.; Wen, L.; Bo, H.; Xin, L.; Chen, Y.; Xu, C.; Pei, Y.; Yang, Y.;

Zhang, X.; Wang, S.; Feng, Z.; Han, J.; Yang, W.; Gao, G. F.; Wu, G.; Li, D.; Wang, Y.; Shu, Y.

Biological features of novel avian influenza A (H7N9) virus. *Nature* **2013,** *499*, 500-503.

(26)   Qi, W.; Jia, W.; Liu, D.; Li, J.; Bi, Y.; Xie, S.; Li, B.; Hu, T.; Du, Y.; Xing, L.; Zhang, J.;

Zhang, F.; Wei, X.; Eden, J. S.; Li, H.; Tian, H.; Li, W.; Su, G.; Lao, G.; Xu, C.; Xu, B.; Liu, W.;

Zhang, G.; Ren, T.; Holmes, E. C.; Cui, J.; Shi, W.; Gao, G. F.; Liao, M. Emergence and

adaptation of a novel highly pathogenic H7N9 influenza virus in birds and humans from a 2013

human-infecting low-pathogenic ancestor. *J. Virol.* **2018,** *92(2) e00921-17*

(27)   Kiso, M.; Kubo, S.; Ozawa, M.; Le, Q. M.; Nidom, C. A.; Yamashita, M.; Kawaoka, Y.

Efficacy of the new neuraminidase inhibitor CS-8958 against H5N1 influenza viruses. *PLoS*

Pathog. **2010,** *6*, e1000786.

(28)   Bantia, S.; Arnold, C. S.; Parker, C. D.; Upshaw, R.; Chand, P. Anti-influenza virus

activity of peramivir in mice with single intramuscular injection. *Antiviral Res.* **2006,** *69*, 39-45.

(29)   Bantia, S.; Upshaw, R.; Babu, Y. S. Characterization of the binding affinities of

peramivir and oseltamivir carboxylate to the neuraminidase enzyme. *Antiviral Res.* **2011,** *91*,

288-291.

(30)   Asaoka, N.; Tanaka, Y.; Sakai, T.; Fujii, Y.; Ohuchi, R.; Ohuchi, M. Low growth ability

of recent influenza clinical isolates in MDCK cells is due to their low receptor binding affinities.

Microbes Infect **2006,** *8*, 511-519.

(31)   Newstead, S. L.; Potter, J. A.; Wilson, J. C.; Xu, G.; Chien, C.-H.; Watts, A. G.; Withers,

S. G.; Taylor, G. L. The structure of Clostridium perfringens NanI sialidase and its catalytic

intermediates. *J. Biol. Chem.* **2008,** *283*, 9080-9088.

(32)   Vavricka, C. J.; Liu, Y.; Kiyota, H.; Sriwilaijaroen, N.; Qi, J.; Tanaka, K.; Wu, Y.; Li, Q.;

Li, Y.; Yan, J.; Suzuki, Y.; Gao, G. F. Influenza neuraminidase operates via a nucleophilic

mechanism and can be targeted by covalent inhibitors. *Nat Comm* **2013,** *4*, 1491.

(33)   Burmeister, W. P.; Henrissat, B.; Bosso, C.; Cusack, S.; Ruigrok, R. W. Influenza B virus

neuraminidase can synthesize its own inhibitor. *Structure* **1993,** *1*, 19-26.

(34)   Winn, M. D.; Ballard, C. C.; Cowtan, K. D.; Dodson, E. J.; Emsley, P.; Evans, P. R.;

Keegan, R. M.; Krissinel, E. B.; Leslie, A. G. W.; McCoy, A.; McNicholas, S. J.; Murshudov, G.

N.; Pannu, N. S.; Potterton, E. A.; Powell, H. R.; Read, R. J.; Vagin, A.; Wilson, K. S. Overview

of the CCP4 suite and current developments. *Acta Crystallogr D* **2011,** *67*, 235-242.

(35)   Varghese, J. N.; Colman, P. M.; van Donkelaar, A.; Blick, T. J.; Sahasrabudhe, A.;

McKimm-Breschkin, J. L. Structural evidence for a second sialic acid binding site in avian

influenza virus neuraminidases. *Proc. Natl. Acad. Sci. U. S. A.* **1997,** *94*, 11808-11812.

(36)   von Itzstein, M.; Wu, W. Y.; Kok, G. B.; Pegg, M. S.; Dyason, J. C.; Jin, B.; Van Phan,

T.; Smythe, M. L.; White, H. F.; Oliver, S. W.; Colman, P. M.; Varghese, J. N.; Ryan, D. M.;

Woods, J. M.; Bethell, R. C.; Hotham, V. J.; Cameron, J. M.; Penn, C. R. Rational design of potent sialidase-based inhibitors of influenza virus replication. *Nature* **1993,** *363*, 418-423.

(37)   McKimm-Breschkin, J. L.; Barrett, S.; Pudjiatmoko; Azhar, M.; Wong, F. Y.; Selleck, P.; Mohr, P. G.; McGrane, J.; Kim, M. I222 neuraminidase mutations further reduce oseltamivir susceptibility of Indonesian Clade 2.1 highly pathogenic avian influenza A(H5N1) viruses. *PLoS One* **2013,** *8*, e66105.

(38)   Uhlendorff, J.; Matrosovich, T.; Klenk, H. D.; Matrosovich, M. Functional significance of the hemadsorption activity of influenza virus neuraminidase and its alteration in pandemic viruses. *Arch. Virol.* **2009,** *154*, 945-957.

(39)   Dai, M.; McBride, R.; Dortmans, J. C.; Peng, W.; Bakkers, M. J.; de Groot, R. J.; van Kuppeveld, F. J.; Paulson, J. C.; de Vries, E.; de Haan, C. A. Mutation of the second sialic acid-binding site, resulting in reduced neuraminidase activity, preceded the emergence of H7N9 influenza A virus. *J. Virol.* **2017,** *91: e00049-17*.

(40)   Hurt, A. C.; Iannello, P.; Jachno, K.; Komadina, N.; Hampson, A. W.; Barr, I. G.; McKimm-Breschkin, J. L. Neuraminidase inhibitor-resistant and -sensitive influenza B viruses isolated from an untreated human patient. *Antimicrob. Agents Chemother.* **2006,** *50*, 1872-1874.

(41)   Mohr, P. G.; Deng, Y. M.; McKimm-Breschkin, J. L. The neuraminidases of MDCK grown human influenza A(H3N2) viruses isolated since 1994 can demonstrate receptor binding. *Virol J.* **2015,** *12*, 67.

(42)   Smith, B. J.; McKimm-Breshkin, J. L.; McDonald, M.; Fernley, R. T.; Varghese, J. N.; Colman, P. M. Structural studies of the resistance of influenza virus neuramindase to inhibitors. *J. Med. Chem.* **2002,** *45*, 2207-2212.

(43)   Otwinowski, Z.; Minor, W. Processing of X-ray diffraction data collected in oscillation

mode. *Methods Enzymol.* **1997**, 307-326.

(44)   McCoy, A. J.; Grosse-Kunstleve, R. W.; Adams, P. D.; Winn, M. D.; Storoni, L. C.;

Read, R. J. Phaser crystallographic software. *J Appl Crystallogr* **2007,** *40*, 658-674.

(45)   Murshudov, G. N.; Vagin, A. A.; Dodson, E. J. Refinement of macromolecular structures

by the maximum-likelihood method. *Acta Crystallogr.* **1997,** *D53*, 240-255.

(46)   McRee, D. E.; Badger, J. MIFit Manual. Version 3.0 for Windows and LINUX. © *Rigaku*

2003-6.

(47)   McRee, D. E. XtalView/Xfit-A versatile program for manipulating atomic coordinates

and electron density. *J Struct Biol* **1999,** *125*, 156-165.

(48)   Brünger, A. T. The Free R value: a novel statistical quantity for assessing the accuracy of

crystal structures. *Nature* **1992,** *355*, 472-474.

(49)   Schrodinger, L. *The PyMOL Molecular Graphics System, Version 1.3r1.,* **2010**.

Table 1 Comparison of 60 min IC$_{50}$ values with (+) and without (-) preincubation

μM	sH1N1 wt	sH1N1 H274Y	pdmH1N1 Cal	pdmH1N1 Shep	H5N1 Cl 1	H5N1 Cl 2	H3N2 wt	H3N2 E119V	H1N9 wt	H1N9 E119G	B wt	B D197E
1-	0.0078	0.0060	0.0120	0.0058	0.0120	0.0112	0.0324	0.0519	0.0057	0.8159	0.1674	0.4338
1+	0.0019	0.0022	0.0011	0.0014	0.0025	0.0013	0.0038	0.0034	0.0027	0.6784	0.0089	0.2575
-/+	4.09	2.72	10.85	4.23	4.71	8.62	8.53	15.26	2.10	1.20	18.81	1.68
2-	0.116	0.139	0.791	0.791	2.168	0.889	1.665	0.465	1.103	1.201	0.414	1.257
2+	0.080	0.116	0.601	0.470	1.662	0.863	1.377	0.238	1.192	1.148	0.065	0.174
-/+	1.45	1.19	1.32	1.68	1.30	1.03	1.21	1.95	0.93	1.05	6.37	7.23
3-	0.048	0.024	0.428	0.474	0.985	0.535	0.313	3.705	0.119	1.278	0.076	0.250
3+	0.069	0.133	0.490	0.490	1.396	0.583	0.318	3.675	0.011	1.050	0.027	0.032
-/+	0.69	0.18	0.87	0.97	0.71	0.92	0.98	1.01	11.23	1.22	2.79	7.75
4-	0.061	0.098	0.457	0.418	0.460	0.281	0.472	0.191	0.438	0.985	0.228	1.550
4+	0.037	0.104[d]	0.330	0.316	0.710	0.316	0.345	0.102	0.289	0.874[d]	0.040	0.212
-/+	1.65	0.95	1.39	1.32	0.65	0.89	1.37	1.88	1.51	1.13	5.76	7.30

5-	8.29	1.15	25.81	25.77	21.66	28.20	28.70	25.14	23.02	132.55	7.62	40.05
5+	2.61	0.28	22.35[d]	21.96[d]	17.05	24.52[d]	5.01	4.40	10.91[d]	107.87[d]	1.15	14.48[d]
-/+	3.17	4.04	1.15	1.17	1.27	1.15	5.73	5.71	2.11	1.23	6.60	2.77
6-	10.76	6.42	31.71	29.64	20.68	23.77	44.57	36.26	25.38	234.81	9.19	79.03
6+	4.50[d]	4.69[d]	20.96	20.68	25.40	26.10	29.51[d]	25.99[d]	22.24[d]	210.19[d]	4.48[d]	32.23[d]
-/+	2.39	1.37	1.51	1.43	0.81	0.91	1.51	1.40	1.14	1.12	2.05	2.45

The IC_{50} values are the means of two individual IC_{50} values for each virus-inhibitor combination.

[a] Virus abbreviations: sH1N1=A/Mississippi/03/01 seasonal (H1N1), pdmH1N1 Cal =pandemic H1N1 A/California/7/09 H1N1, pdmH1N1

Shep =pandemic H1N1 A/Swine/Shepparton/6/2009, H5N1 Cl 1=A/Chicken/Vietnam/08/2004 (H5N1) clade 1, H5N1 Cl 2=

A/Chicken/Bangli/BBVD-563/2007 (H5N1)clade 2, H3N2=A/Fukui/45/04 (H3N2) , H1N9=NWS/G70C H1N9, B=B/Perth/211/2001

[b] - = no preincubation, + = preincubated for 30 min prior to addition of MUNANA substrate,

[c] The greater the difference between no preincubation and preincubation the slower the binding, -/+ ~1 indicates fast, >1.5-2 indicates slow

binding.

[d] IC_{50}s continue to decrease both with and without preincubation (Figures 1 and 2), so the ratio may not properly reflect the extent of slow

binding.

39

Table 2 Time (T½ min) for reaction rates to reach 50% of the maximum rate of the uninhibited control after removal of inhibitor

Virus	Control	1 [19]	2	3	4	5	6
	Ave (SD)	Ave (SD)	Ave (SD)	Ave (SD)	Ave (SD)	Ave (SD)	Ave (SD)
H1N1 A/Mississippi	15.6 (6.3)	41.3 (7.7)[b ***]	24.8 (2.3)[*]	26.7 (0.4)[*]	29.2 (1.6)[**]	30.4 (9.0)[**]	37.5 (4.4)[***]
pdmH1N1 A/Shep	12.5 (3.1)	ND	11.8 (1.6)	11.6 (1.8)	15.8 (0.4)	17.8 (3.7)[**]	24.5 (3.5)[***]
H5N1 Clade 1	15.6 (3.7)	27.7 (2.7)[***]	12.0 (1.1)	13.7 (1.0)	15.0 (2.7)	19.4 (5.5)	17.2 (3.5)
H5N1 Clade 2	12.1 (1.0)	72.8 (5.1)[***]	8.5 (0.5)	10.6 (2.5)	12.3 (2.0)	23.6 (7.7)[***]	16.9 (3.3)[**]
H3N2 A/Fukui	12.8 (3.5)	108.7 (18.8)[***]	17.6 (2.1)[*]	13.4 (4.0)	13.9 (3.8)	25.1 (2.9)[***]	29.7 (7.2)[***]
H1N9 G70C	10.9 (2.1)	32.1 (1.6)[***]	11.1 (0.8)	12.0 (1.1)	13.5 (0.8)	32.2 (1.0)[****]	30.6 (0.6)[***]
B/Perth	10.5 (2.2)	24.6 (3.5)[***]	43.6 (4.2)[***]	29.2 (4.8)[***]	68.7 (14.5)[***]	185.5 (31.9)[***]	>240[***]

Results are from at least two independent assays, with ≥2 replicates per assay.

[a] Virus abbreviations: A/Mississippi =A/Mississippi/03/01 seasonal (H1N1), pdmH1N1 A/Shep =pandemic H1N1 A/Swine/Shepparton/6/2009,

H5N1 Clade 1=A/Chicken/Vietnam/08/2004, H5N1 Clade 2= A/Chicken/Bangli/BBVD-563/2007, H3N2 A/Fukui =A/Fukui/45/04 (H3N2),

H1N9 G70C=NWS/G70C H1N9, B/Perth=B/Perth/211/2001.

40

1
2
3
4
5
6
7
8
9
10
11
12
13
14
15
16
17
18
19
20
21
22
23
24
25
26
27
28
29
30
31
32
33
34
35
36
37
38
39
40
41
42
43
44
45
46
47

[b] The T½ **value** for each inhibitor was compared to the control values by the Student's *t* test, significantly slower compared to control [*]=$P < 0.05$,

[**] $P < 0.01$, [***] $P < 0.001$

41

Table 3 EC$_{50}$s of compounds causing a 50% reduction in plaque size

Virus	1	2	3	4	5	6
	nM	μM	μM	μM	μM	μM
H1N1 A/Mississippi	≤1	1	1	0.1-1	10	10-100
H3N2 A/Fukui	100	100	100	10-100	≥100	ND
H3N2 MDCK A/Victoria	0.1-1	100	10	10	≥100	≥100
H1N9 G70C	1-10	1-10	1-10	10	100	100
B/Perth	10	1	1	1-10	10-100	10-100

A/Mississippi =A/Mississippi/03/01 seasonal (H1N1), H3N2 A/Fukui =A/Fukui/45/04 (H3N2),

A/Victoria =A/Victoria/503/06, H1N9 G70C=NWS/G70C H1N9, B/Perth=B/Perth/211/2001.

Results are from two independent assays.

Table 4.

X-ray data collection and refinement statistics.

	N9 NA -**3**	N9 NA -**4**	N9 NA -**5**	N9 NA -**6**
PDB entry	5W26	5W2U	5W2W	5W2Y
Wavelength (Å)	0.95324	0.95369	0.95324	0.95373
Resolution range (Å)	42.00 – 1.90	48.38 – 2.00	48.30 – 1.85	48.48 – 2.39
	$(1.95 – 1.90)^a$	(2.05 – 2.00)	(1.90 – 1.85)	(2.45 – 2.39)
Space group	I 4 3 2	I 4 3 2	I 4 3 2	I 4 3 2
Unit cell	$a=b=c=180.94$ Å,	$a=b=c=180.03$ Å,	$a=b=c=180.71$ Å,	$a=b=c=181.38$ Å,
	$\alpha=\beta=\gamma=90^o$	$\alpha=\beta=\gamma=90^o$	$\alpha=\beta=\gamma=90^o$	$\alpha=\beta=\gamma=90^o$
Unique reflections	37832 (2735)	32364 (1723)	40605 (2158)	19147 (1035)
Multiplicity	72.0 (25.0)	78.4 (32.0)	75.0 (29.0)	35.4 (16.6)
Completeness (%)	99.9 (99.9)	99.6 (99.8)	99.8 (99.0)	98.5 (98.2)
Mean $I/\sigma(I)$	39.0 (1.5)	10.0 (1.3)	10.2 (1.2)	11.4 (1.8)
Wilson B-factor	22.5	23.1	21.8	22.2
Matthews coefficient, V_m	2.83	2.83	2.83	2.83

43

$(\text{Å}^3/\text{Da})$				
Bulk solvent $k_{sol}(e/\text{Å}^3)$, $B_{sol}(\text{Å}^2)$	0.40, 47.9	0.41, 61.5	0.39, 52.3	0.41, 42.9
R_{merge}[b]	0.170 (0.750)	0.308 (0.760)	0.297 (0.820)	0.394 (0.762)
R_{work}[d]	0.136 (0.289)	0.142 (0.273)	0.140 (0.231)	0.141 (0.257)
R_{free}[e]	0.177 (0.294)	0.187 (0.308)	0.171 (0.262)	0.250 (0.274)
Number of non-hydrogen atoms	3718	3715	3793	3655
macromolecules	3090	3094	3087	3094
ligands	197	197	222	208
water	430	423	483	352
metals	1	1	1	1
Protein residues	388	388	388	388
RMS(bonds) (Å)	0.020	0.021	0.019	0.017
RMS(angles) (°)	2.017	2.078	1.997	1.937
Average B-factor (Å^2)	24.0	25.0	24.0	23.0
Ramachandran favoured (%)	96	96	95	95
Ramachandran allowed (%)	4	4	5	5

44

1
2
3
4
5
6
7
8
9
10
11
12
13
14
15
16
17
18
19
20
21
22
23
24
25
26
27
28
29
30
31
32
33
34
35
36
37
38
39
40
41
42
43
44
45
46
47

[a]Statistics for the highest-resolution shell are shown in parentheses. [b]$R_{\mathrm{merge}} = \sum_{hkl}\sum_j |I_j - <I_j>| / \sum_{hkl}\sum_j | I_j |$, where hkl specifies unique indices, j indicates equivalent observations of hkl, I_j and σ_j^2 are the observed intensities and their errors, and $<Ij>$ and $<\sigma_j>$ are the mean values. [d]$R = \sum_{hkl} || F_o | - F_c | / \sum_{hkl} | F_o|$, where $| F_o |$ and $| F_c |$ are the observed and calculated structure factor amplitudes, respectively. [e]Represents 5% of the data.

45

Figure Legends

Figure 1

Chemical structures of Zanamivir (**1**), 2,3-difluoro sialic acid (DFSA) (**2**), 4-deoxy (**3**), 7-deoxy (**4**), 8-deoxy (**5**) and 9-deoxy (**6**) DFSA.

Figure 2

IC_{50} Kinetics showing changes in IC_{50} values during the 60 min reaction period with (+) or without preincubation (-) for N1 NAs. The IC_{50} value for each 10 min time point is the mean of the individual IC_{50} values of the duplicates for that virus-inhibitor reaction. The greater the difference in final (60 min) IC_{50} values between the reactions without and with preincubation (-/+ ratio), the slower the binding. Additionally, the rate of increase of the IC_{50} values after preincubation with inhibitor upon addition of MUNANA substrate, gives a qualitative indication of the dissociation rate. The faster the increase, i.e. the greater the difference between the 10 min and 60 min IC_{50} values, the faster the dissociation. IC_{50} values for compounds **5** and **6** continue to decrease for some viruses even after preincubation. This novel profile suggests compounds are very slow binding. (A) Seasonal (H1N10 and H274Y mutant, which has reduced sensitivity to oseltamivir and peramivir. (B) pdmH1N1 Cal = human isolate A/California/7/09, Sh=swine isolate A/Swine/Shepparton/6/2009. (C) H5N1 cl 1= A/Chicken//Vietnam/08/2004 clade1, cl 2= A/Chicken/Bangli/BBVD-563/2007 clade 2

Figure 3

IC_{50} Kinetics showing changes in IC_{50} values during the 60 min reaction period with (+) or without (-) preincubation for N2, N9 and B NAs. The IC_{50} value for each 10 min time point is the mean of the individual IC_{50} values of the duplicates for that virus-inhibitor reaction. The

greater the difference in final (60 min) IC_{50} values between the reactions without and with

preincubation (-/+ ratio), the slower the binding. Additionally, the rate of increase of the IC_{50}

values after preincubation with inhibitor upon addition of MUNANA substrate, gives a

qualitative indication of the dissociation rate. The faster the increase, i.e. the greater the

difference between the 10 min and 60 min IC_{50} values, the faster the dissociation. IC_{50} values

for compounds **5** and **6** continue to decrease for some viruses even after preincubation. This

novel profile suggests compounds are very slow binding. (A) H3N2 wild type and E119V

mutant, which has reduced sensitivity to oseltamivir. (B) N9 wild type and E119G mutant,

which has reduced sensitivity to zanamivir. (C) B/Perth wild type and D197E mutant which

has reduced sensitivity to all NAIs.

Figure 4

The N9 NA active site complexes with the trapped covalently bound 3-fluoro-sialyl-enzyme

intermediate in yellow and non-bonded 3-fluoro-oxocarbenium ''transition-state" analogue in

green are shown in the left side panels. The n-deoxy-DFSA (**n=4,7,8,9**) secondary sites are

shown in purple in the right side panels. Red spheres represent water molecules. (A) and (B)

compound **3**; (C) and (D) compound **4**; (E) and (F) compound **5**; and (G) and (H) compound

6, respectively. All sites are overlaid with the omit [34] electron density map shown as a grey

mesh contoured at 1σ within 1.6 Å of ligands. The figure was produced using PyMol.[49]

1
2
3
4
5
6
7
8
9
10
11
12
13
14
15
16
17
18
19
20
21
22
23
24
25
26
27
28
29
30
31
32
33
34
35
36
37
38
39
40
41
42
43
44
45
46
47
48
49
50
51
52
53
54
55
56
57
58
59
60

Figure 1

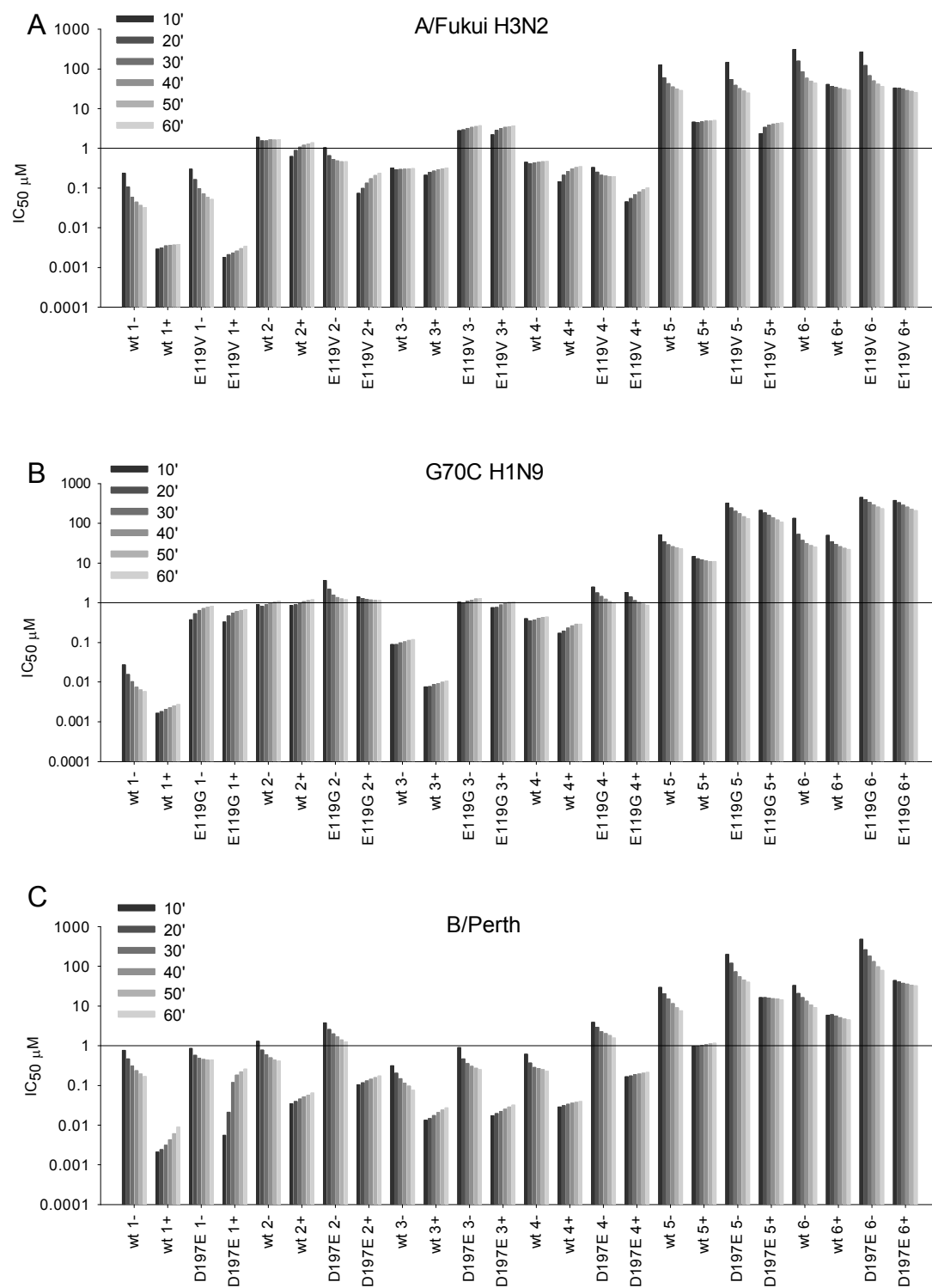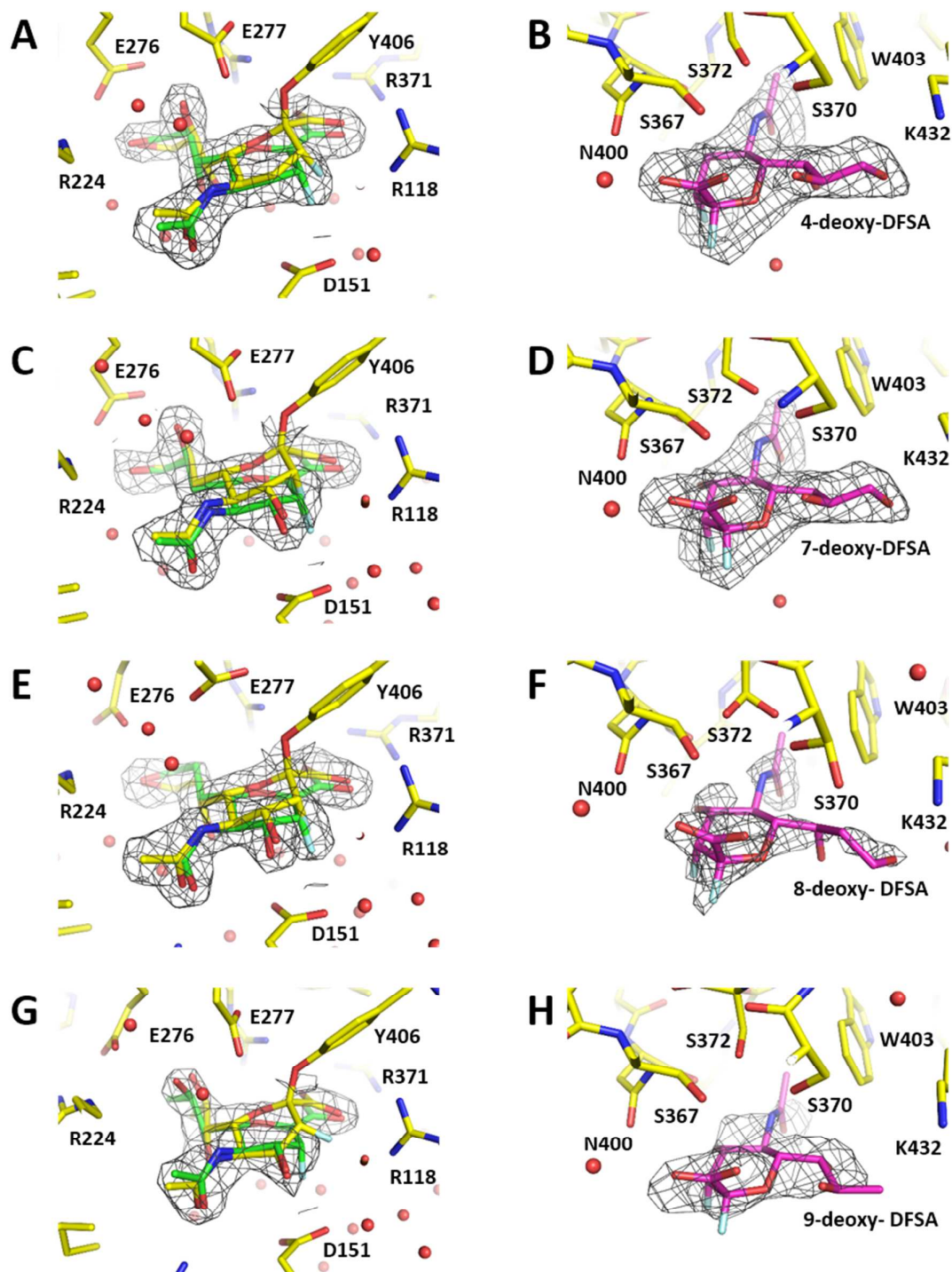Zanamivir (**1**)　　　　(**2**)　　　　(**3**)

(**4**)　　　　(**5**)　　　　(**6**)
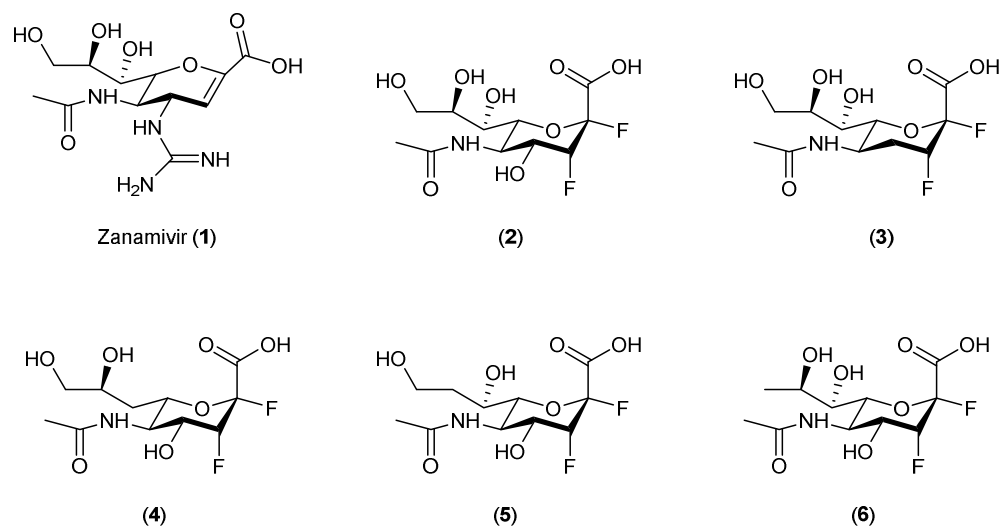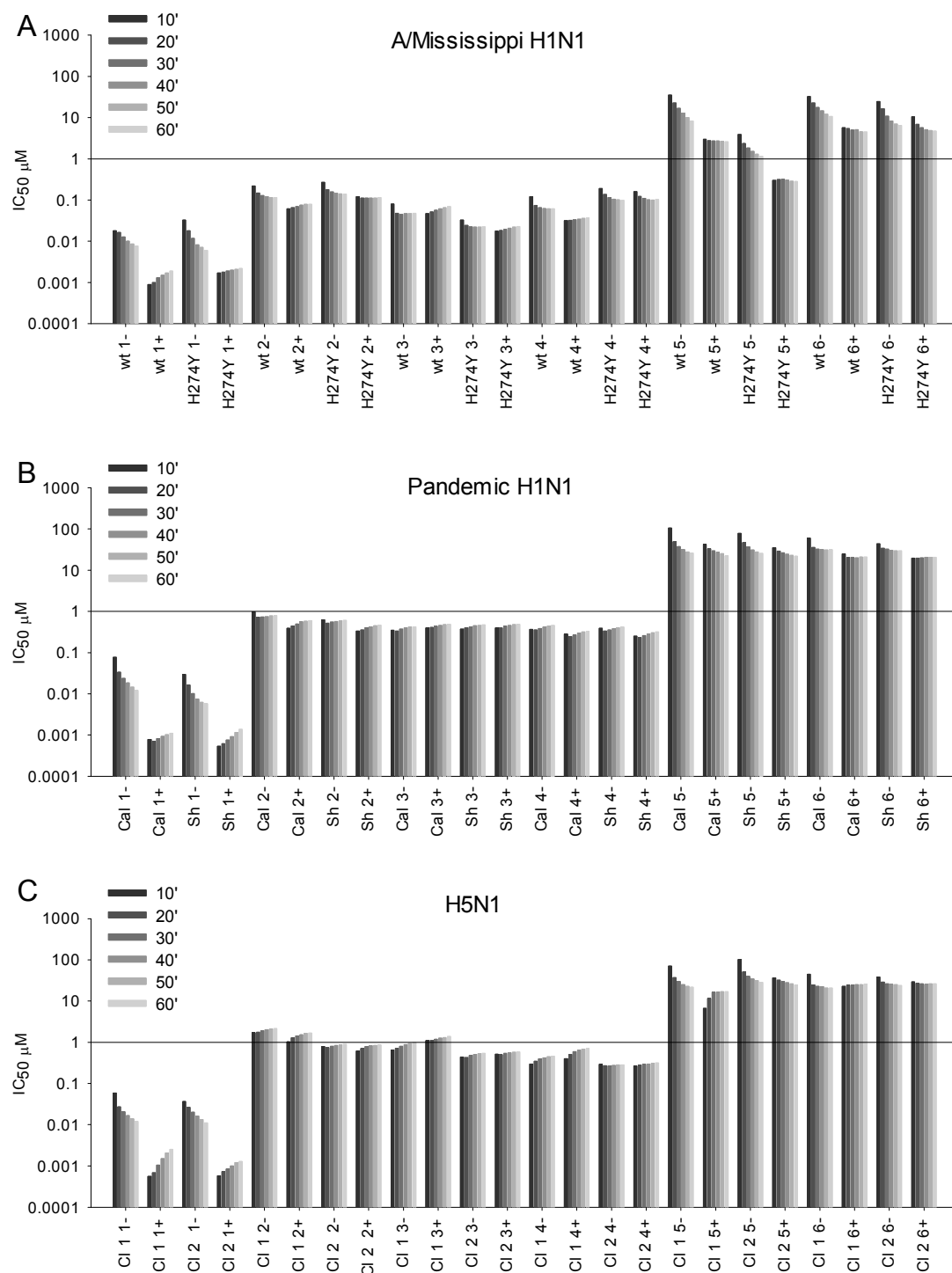
Figure 2

Figure 3

Figure 4

Table of Contents graphic

Decreasing order of turnover, affinity of binding and antiviral potency